Kossel diagram of an aligned cholesteric phase

Richard J. Miller,[1] Helen F. Gleeson,[1,*] and John E. Lydon[2]
[1]*Department of Physics and Astronomy, University of Manchester, Manchester M13 9PL, United Kingdom*
[2]*Department of Biochemistry and Molecular Biology, University of Leeds, Leeds LS29JT, United Kingdom*
(Received 29 July 1997; revised manuscript received 1 September 1998)

The selective reflection of light by the cholesteric phase has been examined using the Kossel technique. The Kossel diagram observed for an aligned monodomain sample, viewed down the helicoidal axis, using crossed polarizers, consists of a single bright annulus. Within this annulus two features are visible—a bright central ring and a pattern of four spiral arcs. When the analyzer is rotated from the crossed to the uncrossed position, one diagonally opposite pair of arcs remains stationary and the other pair rotates around the ring until it becomes superimposed on the stationary pair. The handedness of the spiral pattern is related to the chirality of the phase and offers a direct way of experimentally determining the twist sense—a cholesteric phase with a right-handed twist giving a clockwise spiral pattern. The presence of the more intense central ring and the spiral ''extinction'' pattern are in accordance with the analytical modeling of the selective reflection of cholesteric phases by Oldano *et al.* [S1063-651X(99)02802-0]

PACS number(s): 61.30.Eb

INTRODUCTION

It was the iridescent effects produced by the selective reflection of light by cholesteric phases that prompted the systematic study of thermotropic liquid crystals a century ago [1]. Some indication of the complexity of the optics involved is given by fact that anything approaching a complete analytical treatment of this effect has only recently emerged.

There have been a number of different experimental approaches aimed at understanding the selective reflection of light from cholesteric liquid crystals. The earliest and simplest of these used a ''straight through'' geometry to investigate the light transmitted and reflected normal to the sample, i.e., along the helicoidal axis. Studies of this kind were carried out by Fergason [2] and Adams *et al.* [3] who showed that, under these conditions, the sample acts as a circularly polarizing filter and that an unpolarized incident beam is resolved into two circularly polarized components, one of which is transmitted and the other reflected.

Later investigations examined the situation with single domain samples and with obliquely incident light. For example Berreman and Scheffer [4,5] examined the situation where the incident beam of plane polarized light strikes the specimen at 45° and where the light reflected at 45° is monitored. They varied the temperature and hence the pitch of the cholesteric phase and explored the relationship between wavelength and pitch. They observed the first- and second-order Bragg reflections and found that there was fine detail within these which depended on the polarization conditions. Both reflection bands appeared to be divided into three components (which corresponded to different polarization states) which were more distinctly separated for the second order reflection. Recent more comprehensive treatments of Sugita *et al.* [6] and Takezoe *et al.* [7,8] and Miraldi *et al.* [9,10] and Oldano *et al.* [11,12] explored the effects of varying the pitch, wavelength, incidence angle, polarization state of the incident beam, and a range of analyzer conditions.

In parallel with these experimental investigations there has been a succession of theoretical treatments, dating from the early models of Oseen [13] and de Vries [14] and the subsequent, work of Taupin [15], Fergason [2], and Berreman [3–5]. These theoretical studies culminate with the analytical treatments of Dreher and Meier [16] and Oldano *et al.* and Miraldi *et al.* [9–12]. In these later treatments, the state of the light in the sample is described as a superposition of Bloch wave eigenmodes. Light of a particular frequency and incidence angle will, in general excite four eigenmodes. Each of these represents an elliptically polarized ray traveling through the medium with a periodicity which matches the environment it experiences. However, these modes are paired and within each pair the only difference is that the components of the wave vectors along the helicoidal axis differ in sign while the perpendicular components are the same. Hence for any specific frequency and incidence angle, there are only two truly independent modes. The Oldano approach derives the wave vectors for these two modes.

For each mode there are two possibilities. If the wave vector is real, the mode is stable and is transmitted. Alternatively, if the wave vector is complex the mode is unstable and is reflected. Either of these conditions can apply to either of the two independent modes giving three distinct combinations.

(1) *Both wave vectors are real.* In this case the wave propagates without attenuation, the light is transmitted and there is no reflection.

(2) *One of the wave vectors is real and the other is complex.* One of the modes is therefore transmitted and the other reflected with geometry corresponding to a Bragg reflection.

(3) *Both wave vectors are complex.* (a) If there is no mode mixing, both modes are reflected independently with geometries corresponding to Bragg reflections and all of the incident light is reflected. (b) If there is mixing of the eigenmodes, complete reflection occurs but the geometry does not correspond to Bragg reflection.

*Author to whom correspondence should be addressed. Electronic address: Helen.Gleeson@man.ac.uk

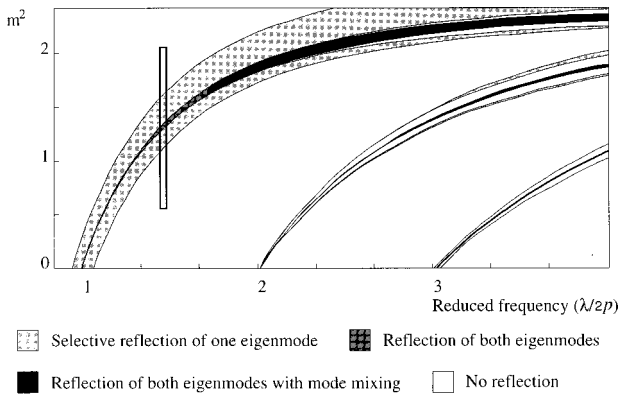

FIG. 1. The Stability chart (redrawn from Oldano *et al.*). The axes in the figure are m ($=n \sin\theta$, where n is the refractive index and θ the angle of incidence) and reduced frequency $2\lambda/p$, where λ is the wavelength and p the pitch of the cholesteric phase. The unshaded region indicates where both modes are transmitted. In the lightly shaded regions one mode is transmitted and the other selectively reflected. In the heavily shaded regions, both modes are reflected. (In the solid black regions both modes are reflected and there is mode mixing.) The region of this chart of relevance to this investigation is shown in the rectangular box.

Both Dreher *et al.* and Oldano *et al.* have laid out the ranges of incidence angles and wavelength for which these various conditions apply on stability charts. The Oldano *et al.* form is shown in Fig. 1.

This paper reports a study of the selective reflection of light from cholesteric liquid crystals using the Kossel diagram technique which is better known in the context of liquid crystals in the study of blue phases. Half a century after their discovery for x rays [17], the optical analogs of Kossel lines were used in the study of the liquid crystal blue phases [18]. Blue phase structures have repeat distances in the visible wavelength range and they selectively reflect light under broadly similar general conditions to those involved in the Bragg reflection of x rays from crystal structures. The Kossel lines given by the blue phases have been used extensively in their study in the examination of their structural symmetries (i.e., their space groups [19,20]), order parameters [21], and the phase of the blue phase structure [22]. In the work presented here we are concerned with the Kossel diagrams produced by aligned cholesteric phases and in particular, the zero-order reflection band at the position indicated by the rectangular box in Fig. 1.

EXPERIMENTAL APPARATUS

The geometry of the Kossel diagram technique employed here is shown in Fig. 2 which also defines the polarization states referred to throughout the paper. The general arrangement of our apparatus is outlined in Fig. 3. Monochromatic light is generated with a laser and then made to converge on the sample using a high numerical aperture objective of a microscope. The selectively reflected light can then be collected using the same objective and the Kossel lines are brought to a focus in the back focal plane. In general, Kossel lines appear as projections of circles onto a plane giving either circles, ellipses or straight lines, depending on the orientation of the corresponding reciprocal lattice vector with respect to the viewing direction. The image created by these lines in the back focal plane is called the Kossel diagram.

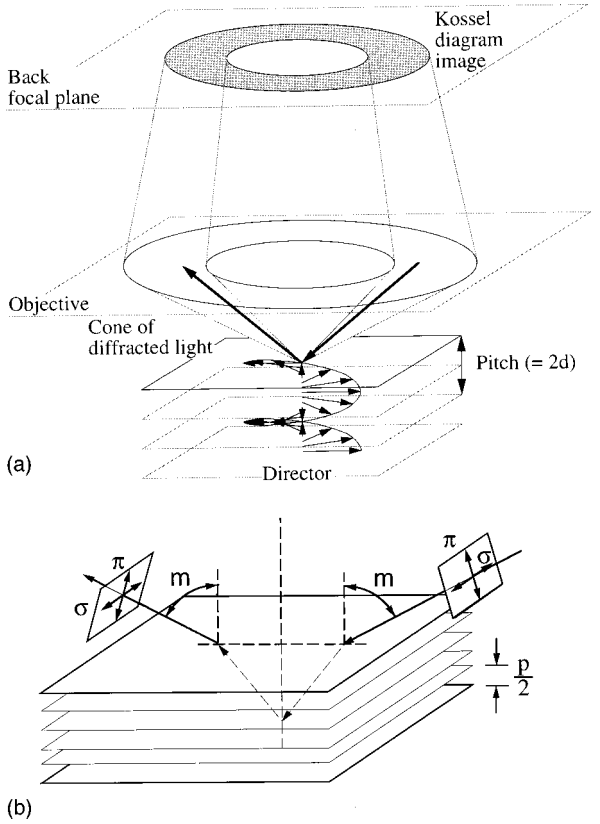

FIG. 2. The geometry of optical Kossel line production. In the Kossel diagram technique a highly convergent beam of light from the laser is incident on the sample. Most of this light passes through the specimen, but rays incident at the Bragg angle are selectively reflected. They are imaged by the objective lens and the Kossel diagram is focused in the back focal plane. In this experiment a single domain cholesteric sample was used with its helicoidal axis parallel to the optic axis of the microscope. (a) To a first approximation the Kossel diagram is a single annular ring showing where the incident and reflected rays are in accordance with a first order Bragg reflection from the periodicity within the specimen. However, the situation is more complex than this and the change of polarization state across the ring gives the fine detail discussed later. (b) defines the polarization directions and angle of incidence in this experiment.

Two lasers were used, a visible laser diode operating at 670 nm and an Ion Laser Technology 450 ASL tuneable Argon laser which gave intense radiation at two wavelengths (488.0 and 514.5 nm). These lasers were coupled to the reflection arm of an Olympus GHMJ metallurgical reflection microscope using a short length of fiber optic bundle. The light was focused onto the sample using an Olympus 100× oil immersion objective with a numerical aperture of 1.3, allowing a wide range of incident angle to be generated. In a sample with refractive index of the order of 1.566, this allows a total angular range of up to 110°. In order to maintain the temperature stability of the sample, the objective was also heated using a Linkam TMS90 temperature controller with a stability of ± 0.01 °C.

The Kossel diagram was imaged using a CCD video camera with resolution of about 640 by 480 pixels. The video

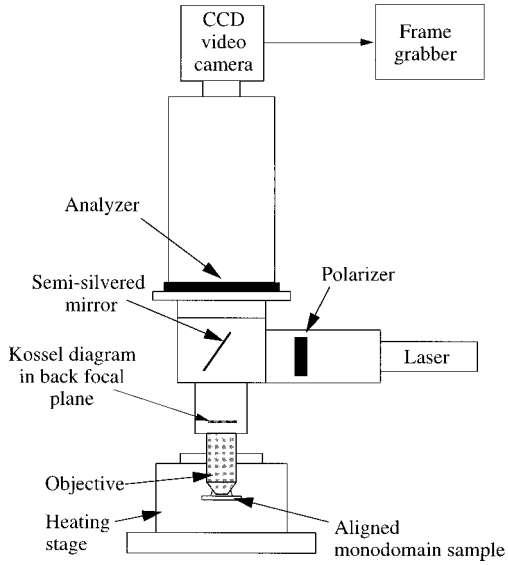

FIG. 3. Apparatus for the production of optical Kossel lines. A sketch showing the principal features of the apparatus used to obtain optical Kossel diagrams. The light from the laser source is reflected in the half-silvered mirror and is focused onto the specimen in a highly convergent beam. The specimen is contained between a glass slide and cover slip.

images were then digitized using a DIPIX Technologies P360F frame grabber [23] and image processing software [24] both installed into 486 IBM-compatible personal computer.

MATERIALS

The commercially available thermochromic mixture TM533 (Merck UK Ltd.) [25] was used. This provided a convenient temperature-dependent cholesteric phase which reflected across the whole visible spectrum. The sample was held between a glass slide and cover slip which had been treated with polyvinyl alcohol (PVA) and rubbed to produce a planar alignment. The sample was approximately 10-μm thick.

RESULTS

The Kossel diagrams obtained are shown in Fig. 4. The most striking feature of these diagrams is the detail visible within the annulus; the central more intense ring and the superposed darker spiral bands on both the inner and outer parts of the annulus. The detail observed within the annulus was dependent on the polarization state of the incident and detected light. When a polarizer, but no analyzer, was used, a single pair of dark spiral arms was seen. When crossed polarizers were used, a pattern of four spiral arcs was seen and this pattern was found to rotate bodily when the crossed polarizers were rotated together. If the polarizer was held stationary and the analyzer rotated on its own out of the crossed position, one pair of the spirals on opposite sides of the ring, remained stationary and the other pair rotated in the same sense as the analyzer and ultimately merged with the stationary pair when the two polarizers were in the parallel position.

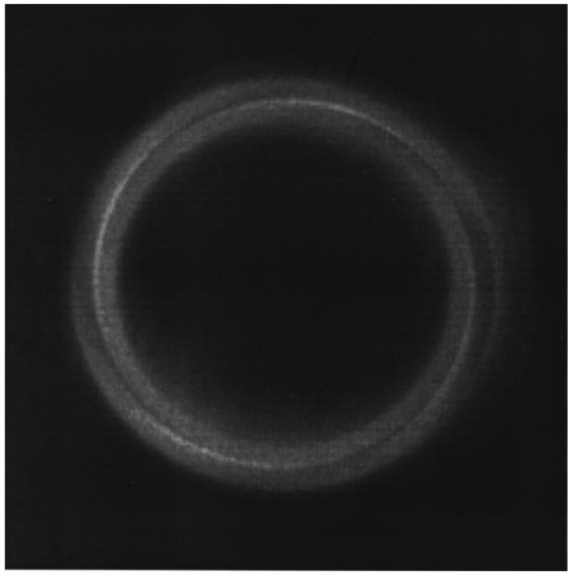

FIG. 4. The observed Kossel diagram. A Kossel diagram of the commercial thermochromic material TM533 at a temperature of 1.4 °C above the smectic-$A\rightarrow$cholesteric phase transition, obtained with crossed polarizers. Note the features within the annular ring, the brighter central ring, and the pattern of four spiral arcs superimposed on both inner and outer regions of the annulus.

DISCUSSION

The data obtained in our experiment using the Kossel technique corresponds to the region of the stability chart noted in Fig. 1. In this region of the stability chart, the first-order reflection band has a relatively narrow central part where both modes are reflected, and broader, more or less symmetrical areas where there is reflection of only one of the two modes. At first sight therefore, we would expect, the intensity profile across a reflection to have the form shown in Fig. 5(a) with a central, relatively sharp spike with flat shoulders. For unpolarized incident light and with no analyzer, this is more or less the case, but when linear or circular polarizers and/or analyzers are used the situation is more complex because of the change in polarization state across the reflection band. For example, if the σ-π geometry is used we would expect an intensity profile of the form shown in Fig. 5(b).

The intensity with which the possible modes are excited depends on the polarization state of the incident light and if an analyzer is inserted, the portion of the reflected light which passes through it depends on its type (i.e., linear or circular) and orientation. There is therefore a wide variety of possible experimental conditions which can be explored. Some of these are described in the paper by Miraldi *et al.* [12]. The situations which are of concern here involve linearly polarized incident light with the two orthogonal polarization directions σ and π as defined in Fig. 2. The intensity profiles across the reflection bands when observed with a polarizer but no analyzer for these two conditions are shown in Fig. 6(a). The corresponding situations with plane-polarized analyzers added in the crossed and uncrossed positions are shown in Figs. 6(b) and 6(c). The two profiles shown in Fig. 6(b) correspond to the two perpendicular sections across the observed Kossel annulus shown in Fig. 7 at

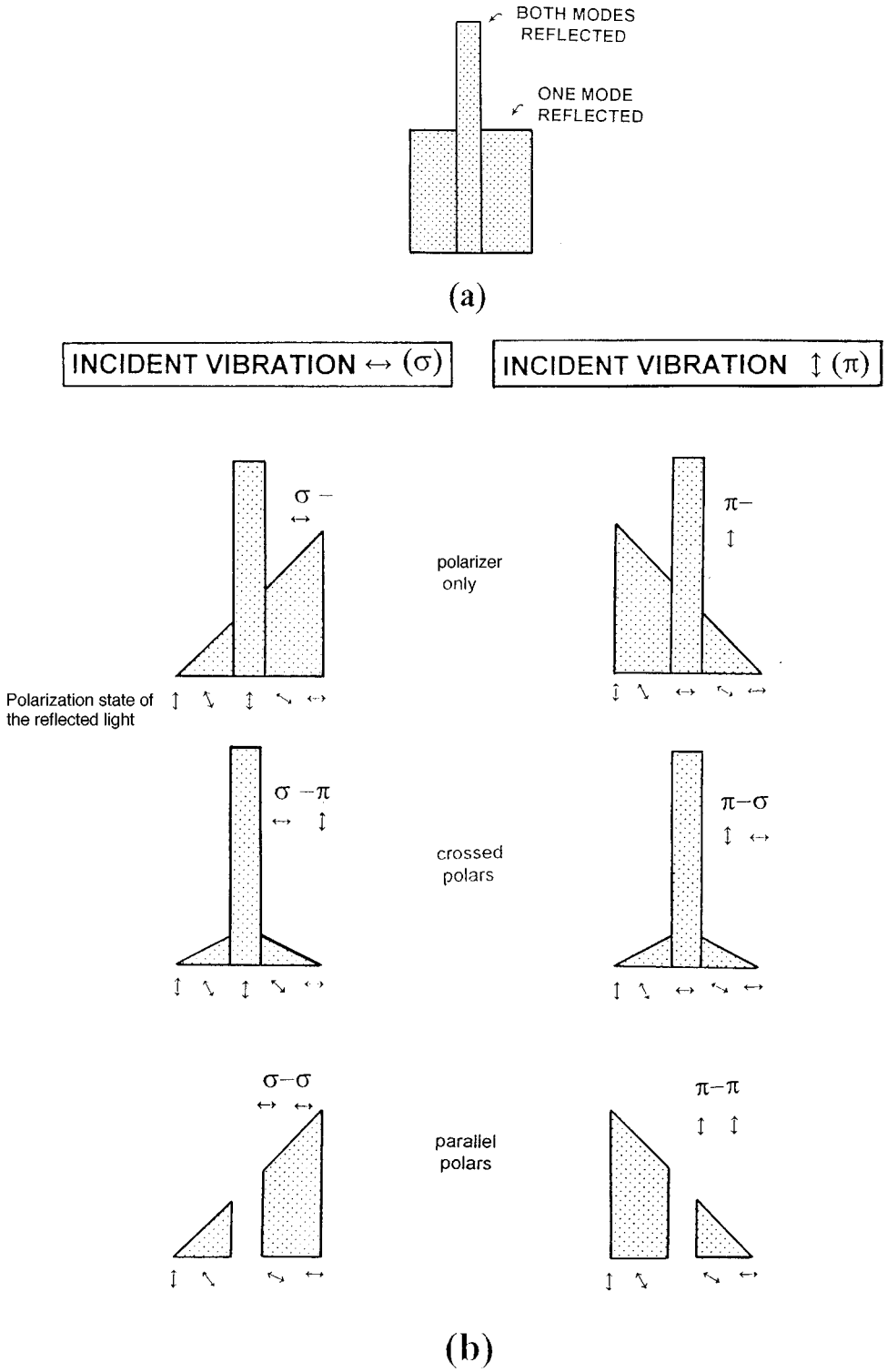

FIG. 5. The intensity profile of the reflection band. At a position corresponding to the rectangular box drawn on Fig. 1 the zero-order reflection band has two parts: the central region where both modes are selectively reflected and the shoulders where only one mode is reflected. At first sight, one might expect the intensity profile across the band to have the form shown in (a) with a central peak and two shoulders of equal intensity. However, as sketched in (b), because of the change of polarization state across the band and because the central two mode region has a different polarization state to the adjoining parts of the one mode regions (indicated at the bottom of each sketch), the observed intensity profile is more complex and depends on the orientations of the polarizer and analyzer used. For incident plane polarized light, the observed intensity is a function of the modes excited by the incident light and the components selectively transmitted by the analyzer. The intensity profiles expected for linear polarizers alone (i.e., with no analyzers) are shown in the sketches labeled σ- and π-. The profiles expected for combinations of crossed and parallel polarizers are shown in the sketches labeled π-σ, π-π and σ-π, σ-σ. Note that the incident plane polarized light excites the central two mode band in the orthogonal sense, i.e., σ excites π and conversely π excites σ. In practice the situation is further complicated by the fact that the sample is a finite number of pitches thick. This has the effect of modulating the experimentally observed profiles giving traces of the form shown in Fig. 6.

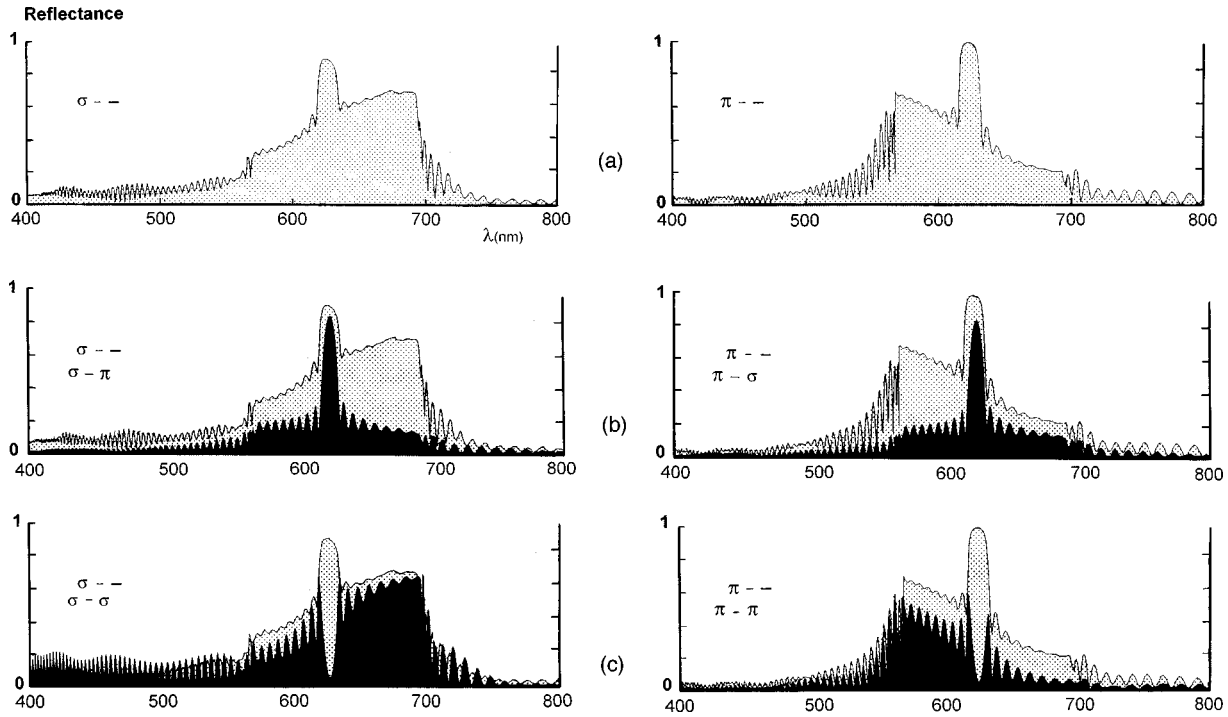

FIG. 6. Results of the Miraldi *et al.* study. These six figures have been redrawn from the paper by Miraldi *et al.* [12]. These workers obtained a remarkable level of correspondence between the experimental and theoretical intensity profiles with the two sets of patterns being virtually indistinguishable. Note that the sinusoidal modulation of these profiles is a function of the thickness of the experimental sample cell. The number of pitches of the helicoidal structure in the sample thickness (which was constrained to be an integer or half integer, because of the epitaxial alignment of the upper and lower surfaces of the sample) was the only parameter allowed to refine in their treatment. (a) Profiles of the intensity across the (first-order) reflection band using incident plane-polarized light and no analyzer. The π and σ directions are as defined in Fig. 2. (b) Intensity profiles for crossed polarizers in the σ-π and π-σ geometries. These correspond to the sections of the Kossel annulus shown in Fig. 7 at the 9 o'clock and 12 o'clock positions, respectively. (c) Profiles for uncrossed polarizers in the π-π and σ-σ geometries. These correspond to the sections of the Kossel annulus shown in Fig. 8(a) at the 9 o'clock and 12 o'clock positions, respectively.

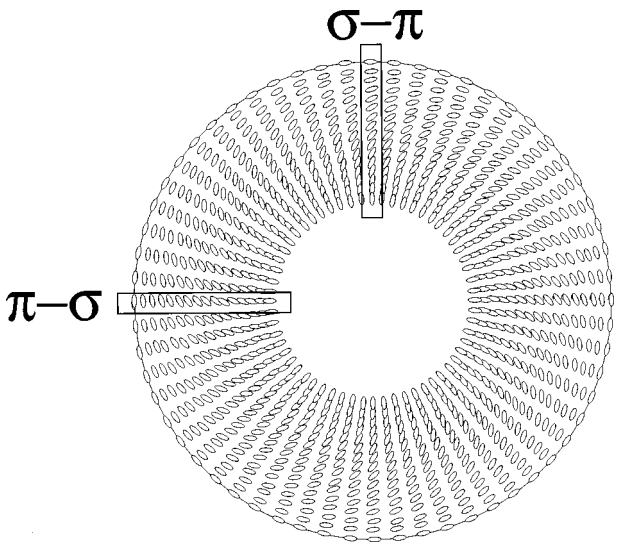

FIG. 7. The origin of the spiral arm pattern. This diagram shows the polarization state at different parts of the Kossel ring. For clarity, the central, more intense band (corresponding to the region where both modes are reflected) has been omitted. For crossed polarizers the combined effect of the components of the modes not excited by the incident beam and the components subsequently removed by the analyzer gives rise to the pattern of four spiral arms. The regions within the rectangular boxes correspond to separate experimental (and theoretical) investigations with crossed polarizers by Oldano *et al.* shown in Fig. 6(b).

the 9 o'clock and 12 o'clock positions. The two profiles shown in Fig. 6(c) correspond to similar sections across the Kossel annulus shown in Fig. 8(a). Note that for a plane-polarized incident beam the central region of the reflection band is plane polarized in an orthogonal sense to the incident beam (i.e., π excitation gives a σ polarized central band and conversely σ excitation gives a π central zone).

The central bright ring. The central, more intense ring, occurs where both modes are reflected. One would therefore expect to find that the profile of the reflection observed would have the simple two step form shown in Fig. 5(a) and the annular ring would have a more intense central band. This is more or less the case, but the situation is complicated by the polarization state of the light. If crossed polarizers are used, spiral ''shadows'' are superimposed on both the central ring and on the outer part of the annulus as discussed below.

The spiral pattern. In general, the light selectively reflected by the cholesteric structure is elliptically polarized. According to the treatment of Oldano *et al.* the orientation of the major axis of the ellipse rotates as we traverse the reflection band, from a radial alignment on the inside, to a tangential alignment on the outside, as shown in Fig. 7. This figure explains both the spiral detail obtained using crossed polarizers and the change in appearance of the spiral pattern when the analyzer is rotated. There are two stages in this explanation.

(1) It is only when the incident beam is unpolarized that the elliptical modes can be fully excited. If the incident beam

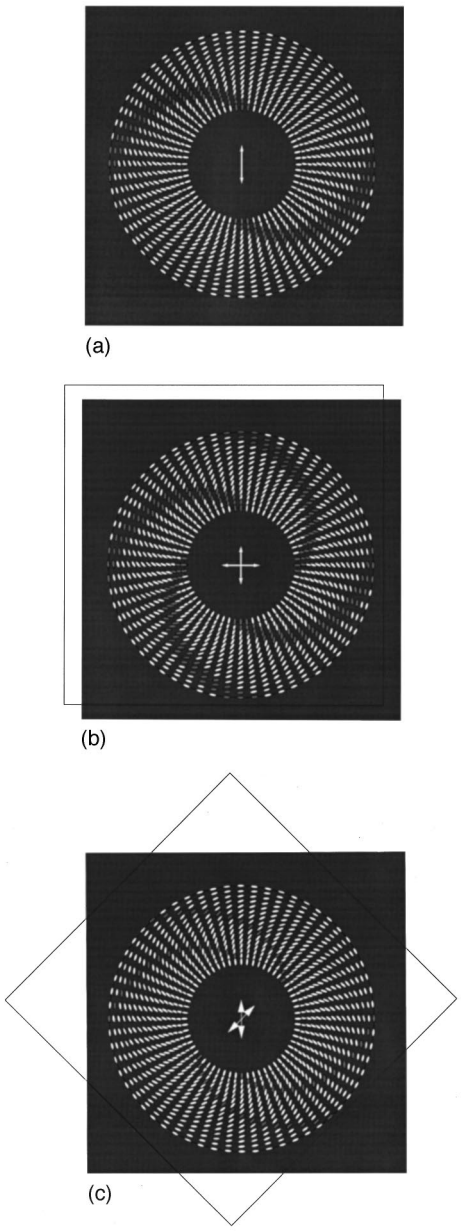

FIG. 8. The effect of uncrossing the polarizers. If the analyzer is rotated from the crossed to the uncrossed position, one opposite pair of spiral arms remains stationary and the other rotates until it becomes superimposed on the stationary pair. (a) A representation of the modes excited when the incident beam is plane-polarized (with no analyzer). The 9 o'clock and 12 o'clock radii correspond to the separate experimental and theoretical investigations by Miraldi *et al.* for the σ and π situations, respectively, shown in Fig. 6(a). (b) The modes transmitted with crossed polarizer and analyzer. The 9 o'clock and 12 o'clock radii correspond to the conditions shown in Fig. 6(b) with π-σ and σ-π geometries, respectively. (c) The modes transmitted with polarizer and the analyzer in the 45° position.

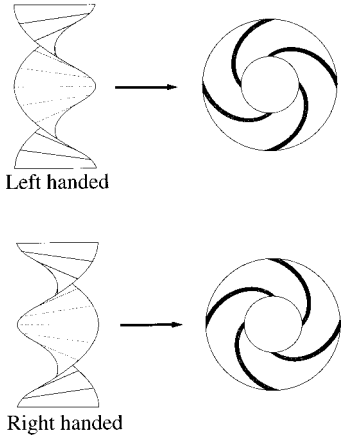

FIG. 9. The relationship between the chirality of the cholesteric phase and the sense of the spiral pattern within the Kossel annulus observed crossed polarizers. A left-handed cholesteric phase gives a Kossel pattern which spirals outwards in an anticlockwise sense whereas a right-handed cholesteric phase gives a Kossel pattern which spirals outwards in a clockwise sense. The Kossel technique therefore offers a direct method for determining the handedness of a cholesteric phase in contrast to the classical method which involves the formation of compensated mixtures with cholesteric phases of the opposite chirality.

is plane polarized, some of the components are missing. It can be seen from Fig. 8(a) that the locus of the positions where the major axis has a particular orientation (vertical in this sketch) is a pattern of two spiral arms. The annulus observed using a plane polarizer and no analyzer, therefore contains two dark spiral arms, indicating the regions where the horizontal components have not been excited.

(2) If an analyzer in the crossed position is used, then the horizontal components of the array are extinguished and the pattern of four spiral arms is created, Fig. 8(b). If the analyzer is rotated out of the crossed position, one pair of arms rotates as shown in Fig. 8(c) until, when the parallel position is reached, the spiral arcs become superimposed.

If we ignore the central, more intense band (corresponding to the region where both modes are reflected), the pattern observed for parallel polarizers is the same as the pattern observed using the polarizer alone.

The relationship between the handedness of the cholesteric twist and the sense of the spiral arc pattern. The sense of the spiral arc pattern (i.e., whether it spirals outwards in a right-handed or left-handed way) depends in the way in which the polarization state changes across the reflection band and this is a consequence of the handedness of the cholesteric phase. In order to determine how the sense of the spiral detail within the Kossel ring is related to the handedness of the cholesteric sample, the classical ''compensated mixture'' method was used. A contact preparation of TM533 was made with the Merck chiral dopant C15. The latter forms a left-handed cholesteric phase when mixed with nonchiral nematic phases. It was found to cause the pitch of the TM533 to increase, i.e., it unwinds the helicoidal structure. Hence we infer that the TM533 mesophase is right-handed. It appears that right-handed cholesteric phases give Kossel rings in which the detail spirals outwards in a clockwise sense and conversely, left-handed cholesteric phases would be expected to give patterns which spiral outwards in an anti-clockwise sense. (This relationship must be implicit in the Dreher and Oldano treatments and we intend to explore it in a future publication.) The Kossel diagram therefore offers a direct and totally unambiguous way of determining the handedness of a cholesteric phase (which does not make any assumptions about the behavior of chiral dopants), a right-

handed cholesteric phase giving a left-handed spiral pattern (Fig. 9).

CONCLUSION

The Kossel diagram obtained from an aligned sample of the cholesteric phase viewed with crossed polarizers, is a single annular ring. Within this ring there are two features, a central ring, and a pattern of spiral arcs. Both of these features are compatible with the analytical treatment of the selective reflection of light from helicoidal structures by Oldano *et al.* The relationship between the handedness of the spiral pattern and the chirality of the cholesteric phase offers a direct way of determining the sense of twist of a cholesteric phase.

ACKNOWLEDGMENTS

The authors would like to thank the EPSRC and the MOD for financial support (Grant No. GR/H/95860), and William Deakin for useful and enthusiastic discussions.

[1] F. Reinitzer, Monatsch. Chem. **9**, 421 (1888).
[2] J. L. Fergason, Mol. Cryst. Liq. Cryst. **1**, 293 (1966).
[3] J. E. Adams, W. Haas, and J. Wysochi, J. Chem. Phys. **50**, 2458 (1969).
[4] D. W. Berreman and T. J. Scheffer, Phys. Rev. Lett. **25**, 577 (1970); Mol. Cryst. Liq. Cryst. **11**, 395 (1970).
[5] D. W. Berreman, J. Opt. Soc. Am. **62**, 502 (1972).
[6] A. Sugita, H. Takezoe, Y. Ouchi, A. Fukuda, E. Kize, and N. Goto, Jpn. J. Appl. Phys. **21**, 1543 (1982).
[7] H. Takezoe, Y. Ouchi, A. Sugita, M. Hara, A. Fukuda, and E. Kuze, Jpn. J. Appl. Phys. **21**, 1390 (1982).
[8] H. Takezoe, Y. Ouchi, A. Sugita, M. Hara, A. Fukuda, and E. Kuze, Jpn. J. Appl. Phys. **22**, 1080 (1983).
[9] E. Miraldi, C. Oldano, P. Taverna Valabrega, and L. Trossi, Mol. Cryst. Liq. Cryst. **103**, 155 (1983).
[10] E. Miraldi, C. Oldano, P. Taverna Valabrega, and L. Trossi, Jpn. J. Appl. Phys. **23**, 802 (1984).
[11] C. Oldano, E. Miraldi, and P. Taverna Valabrega, Phys. Rev. A **27**, 3291 (1983).
[12] C. Oldano, Phys. Rev. A **31**, 1014 (1985).
[13] C. W. Oseen, Ark. Mat., Astron. Fys. **21A**, 14 (1928); **21A**, 1 (1929); Trans. Faraday Soc. **29**, 883 (1933).
[14] H. de Vries, Acta Crystallogr. **4**, 219 (1951).
[15] D. Taupin, J. Phys. C **30**, 32 (1969).
[16] R. Dreher and G. Meier, Phys. Rev. A **8**, 1616 (1973).
[17] W. Kossel, V. Loeck, and H. Voges, Z. Phys. **94**, 139 (1935).
[18] P. E. Cladis, T. Garel, and P. Pieranski, Phys. Rev. Lett. **57**, 2841 (1986); B. Jérôme and P. Pieranski, Liq. Cryst. **5**, 799 (1989); G. Heppke *et al.*, J. Phys. (France) **50**, 549 (1989).
[19] S. Meiboom and M. Sammon, Phys. Rev. A **24**, 468 (1981); D. L. Johnson *et al.*, Phys. Rev. Lett. **45**, 641 (1980); G. Heppke *et al.*, J. Phys. (France) **50**, 549 (1989).
[20] R. J. Miller, J. E. Lydon, and H. F. Gleeson, J. Phys. (France) **6**, 909 (1996).
[21] R. J. Miller, J. E. Lydon, and H. F. Gleeson, Phys. Rev. E **52**, 5011 (1995).
[22] R. J. Miller, H. F. Gleeson, and J. E. Lydon, Phys. Rev. Lett. **77**, 857 (1996).
[23] DIPIX Technologies Inc., 1050 Baxter Road, Ottawa, Ontario, Canada.
[24] Accuware version 2.4, Automated Visual Inspection, 2519 Palmdale Court, Santa Clara, CA 95051.
[25] Merck, Ltd., Merck House, Poole, Dorset, United Kingdom.